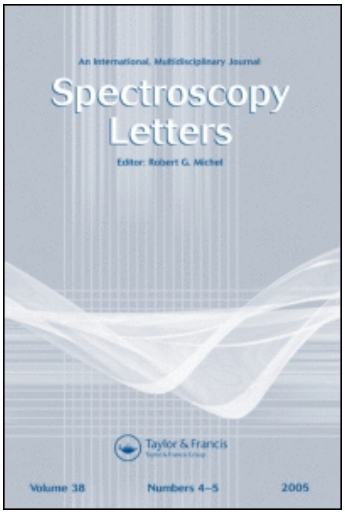

Spectroscopy Letters

Publication details, including instructions for authors and subscription information:
http://www.informaworld.com/smpp/title~content=t713597299

Characterization and Spectral Study of 1,4-Dimethylquinoxaline-2,3-dione Potassium Iodide Complex

B. Benali[a]; Z. Lazar[a]; A. Boucetta[a]; A. El Assyry[a]; B. Lakhrissi[b]; M. Massoui[b]; C. Jermoumi[b]; P. Negrier[c]; J. M. Leger[d]; D. Mondieig[c]

[a] Département de Physique, Faculté des Sciences, Laboratoire d'Opto-électronique et de Physico-Chimie des Matériaux, Kénitra, Morocco [b] Département de Chimie, Faculté des Sciences, Laboratoire de Chimie des Agroressources, Kénitra, Morocco [c] Centre de Physique Moléculaire Optique et Hertzienne, Université Bordeaux 1, Talence, France [d] Laboratoire de Pharmacochimie, Université Victor Segalen Bordeaux 2, Bordeaux, France

To cite this Article Benali, B. , Lazar, Z. , Boucetta, A. , Assyry, A. El , Lakhrissi, B. , Massoui, M. , Jermoumi, C. , Negrier, P. , Leger, J. M. and Mondieig, D.(2008) 'Characterization and Spectral Study of 1,4-Dimethylquinoxaline-2,3-dione Potassium Iodide Complex', Spectroscopy Letters, 41: 2, 64 — 71

To link to this Article: DOI: 10.1080/00387010801943525

URL: http://dx.doi.org/10.1080/00387010801943525

Spectroscopy Letters, 41:64–71, 2008

ISSN: 0038-7010 print/1532-2289 online
DOI: 10.1080/00387010801943525

Taylor & Francis
Taylor & Francis Group

Characterization and Spectral Study of 1,4-Dimethylquinoxaline-2,3-dione Potassium Iodide Complex*

B. Benali,[1] Z. Lazar,[1] A. Boucetta,[1] A. El Assyry,[1] B. Lakhrissi,[2] M. Massoui,[2] C. Jermoumi,[2] P. Negrier,[3] J. M. Leger,[4] and D. Mondieig[3]

[1]Faculté des Sciences, Laboratoire d'Opto-électronique et de Physico-Chimie des Matériaux, Département de Physique, Kénitra, Morocco

[2]Faculté des Sciences, Laboratoire de Chimie des Agroressources, Département de Chimie, Kénitra, Morocco

[3]Centre de Physique Moléculaire Optique et Hertzienne, Université Bordeaux 1, Talence, France

[4]Laboratoire de Pharmacochimie, Université Victor Segalen Bordeaux 2, Bordeaux, France

Received 2 October 2006; accepted 22 January 2008.

*The authors were invited to contribute this paper to a special issue of the journal entitled "Research on Spectroscopy in Morocco." This special issue was organized by Miguel de la Guardia, Professor of Analytical Chemistry at Valencia University, Spain, and the first group of papers was published in *Spectroscopy Letters*, 40(5), 2007. This article is grouped with other Moroccan papers in volume 41(2), 2008.

Address correspondence to B. Benali, Faculté des Sciences, Laboratoire d'Opto-électronique et de Physico-Chimie des MatériauxDépartement de Physique, Kénitra, Morocco. E-mail: benali_bouziane@yahoo.fr

ABSTRACT 1,4-Dimethylquinoxaline-2,3-dione potassium iodide complex was prepared, and its structure was determined by single crystal X-ray diffraction. Elsewhere, solvent effects on the energy of excited and ground states of the complex in solution have been investigated by absorption and fluorescence spectroscopy. The change displayed by the photophysical properties of this complex in different solvents can be explained in terms of a sum of dielectric and hydrogen bonding effects taking part in the stabilization or destabilization of the structure

KEYWORDS 1,4-dimethylquinoxaline-2,3-dione potassium iodide complex, dipole–dipole and hydrogen bond interactions, electronic absorption, fluorescence, single crystal structure, synthesis

1. INTRODUCTION

1,4-Dimethylquinoxaline-2,3-dione is composed of a phenyl ring condensed with a six-membered heterocyclic (Fig. 1). We were interested in the molecular properties of the 1,4-dimethylquinoxaline-2,3-dione potassium iodide complex as several publications recently indicated that some quinoxaline-2,3-dione derivatives have been studied because of their biological and pharmacological activities.[1–4] Renewed interest arises from the discovery that disubstituted derivatives, notably 6,7-dinitro and 6-cyano-7-nitro, are potent antagonists of the quisqualate and kalnate receptors on neurons of the central nervous system.[5–7]

Because of this pharmacological interest, and in the absence of fundamental spectroscopic data in the literature on this quinoxaline-2,3-dione complex, we considered it useful to discuss some of their molecular properties of potential interest. These could explore the reactivity and mechanisms of quinoxaline-2,3-dione in biological systems like those mentioned above. The purpose here was to synthesize and study the structure of the complex by X-ray diffraction analysis and to observe its spectral behavior in various solvents.

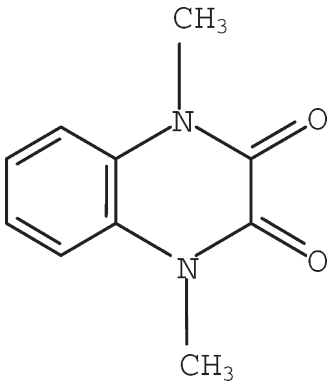

FIGURE 1 **Chemical Diagram of 1,4-Dimethylquinoxaline-2,3-Dione.**

2. MATERIALS AND METHODS

2.1. Preparation of the Complex

Quinoxaline-2,3-dione precursor was synthesized according to a method described elsewhere.[8] To ortho-phenylenediamine (1 g, 0.01 mole) dissolved in HCl (4 N, 20 mL) was added dehydrate oxalic acid (1.17 g, 0.017 mole). The mixture was heated for 10 min and the resulting precipitate was collected by filtration and washed three times with water then recrystallized from methanol. The product was isolated as a white solid with 90% yield, m.p. 250–352°C; IR (KBr): υ(C═O) = 1770 cm^{-1}, υ(NH) = 3400 cm^{-1}; ^{1}H NMR (300 MHz, $DMSOd_6$): δ ppm: 7.05 (4H, m, CH-aromatic); 11.87 (2 H, S, NH); ^{13}C NMR (75 MHz, $DMSOd_6$): δ ppm according to the atoms classification in Figure 2: δ ppm: 115.10 [C-aromatic (C2;C5)]; 115.50 [C-aromatic (C3;C4)]; 122.68 [C-quaternary (C1;C6)]; 155.15[C-quaternary (C8;C9)].

The quinoxaline-2,3-dione was identified by NMR ^{1}H, ^{13}C, IR, and by comparison of its physical characteristics with those of the literature[9] 1,4-dimethyl-quinoxaline-2,3-dione.

The 1,4-dimethylquinoxaline-2,3-dione potassium iodide complex was obtained by the reaction of quinoxaline-2,3-dione in dimethylformamide using methyl iodide in the presence of potassium carbonate and tetrabutylammonium bromide at room temperature.

Potassium carbonate (0.03 mole) was dispersed in 60 mL dimethylformamide, and quinoxaline-2,3-dione (0.01 mole) was added to this mixture. The solution was stirred for 1 h; afterward, 0.03 mole of methyl iodide and 0.001 mole of tetrabutylammonium bromide were added. The mixture was stirred for 6 h at room temperature. Then the mixture was filtered, and the filtrate was left at room temperature for 10 h. The resulting precipitate was filtered and dried. Figure 2b shows the IR spectrum of the complex indicating some intensity bands and compared with those observed in the IR spectrum of the 1,4-dimethylquinoxaline-2,3-dione. This comparison suggests the existence of the 1,4-dimethylquinoxaline-2,3-dione potassium iodide complex.

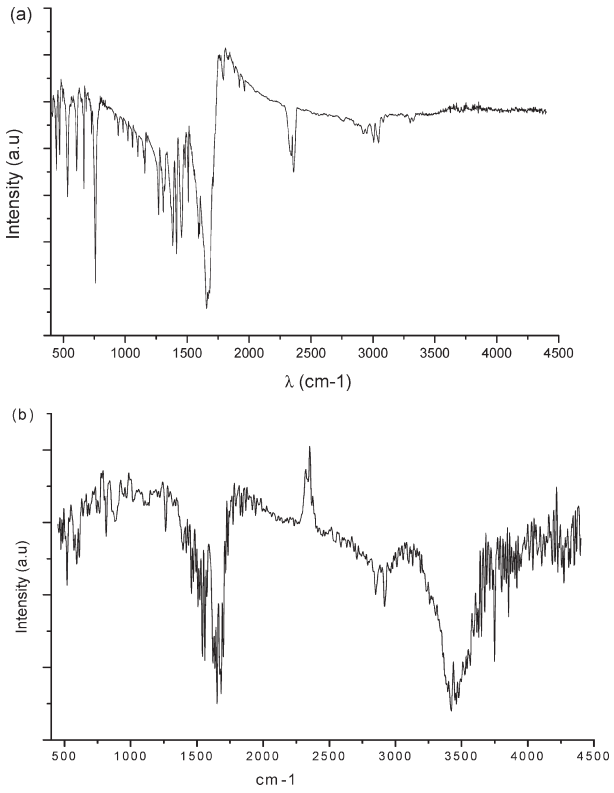

FIGURE 2 **IR Spectra of the 1,4-Dimethylquinoxaline-2,3-dione (a) and the Complex (b).**

2.2. Crystallographic Data Collection and Structure Analysis

An uncolored single crystal (0.25 mm × 0.10 mm × 0.10 mm) was selected and mounted on an ENRAF-NONIUS CAD4 diffractometer equipped with a charge-coupled device (CCD) detector using Cu-Kα X-ray radiation (λ = 1.054180 Å). 1329 reflections were collected in the 4.86° to 64.99° theta range. The details of data collection are given in Table 1. The structure was solved by direct methods. The non-hydrogen atoms were located from the difference Fourier maps and further refined anisotropically by full-matrix least squares to final reliability values of 0.04. All

TABLE 1 Crystal Data and Structure Refinement for the Complex

Empirical formula = C_{10} H_{10} $I_{0.50}$ $K_{0.50}$ N_2 O_2; Formula weight = 273.20 g
Crystal system: orthorhombic; space group: P b c n, Z = 8
Unit cell dimensions: a = 18.206(4) Å, b = 7.094(5) Å, c = 16.385(2) Å
Volume:2116.2(16) $Å^3$, Calculated density: 1.715 g cm^{-3}
Absorption coefficient: 13.953 mm^{-1}
F(000) = 1088
Crystal size: 0.25 × 0.10 × 0.10 mm
Theta range for data collection: 4.86° to 64.99°
Limiting indices: $0 \le h \le 21$, $0 \le k \le 5$, $0 \le l \le 19$
Reflections collected/unique: 1329/1329 [R(int) = 0.0000]
Completeness to theta = 64.99, 73.8%
Max and min transmission: 0.3359 and 0.1281
Refinement method = full-matrix least-squares on F2
Data/restraints/parameters: 1329/0/140
Goodness-of-fit on F^2 = 1.114
Final R indices [I > 2sigma(I)]: R1 = 0.0309, w_{R2} = 0.0839
R indices (all data): R1 = 0.0427, w_{R2} = 0.0926
Extinction coefficient: 0.00218(14)
Largest diff. peak and hole: 0.686 and −0.416 e $Å^{-3}$

TABLE 2 Atomic Coordinates (×10^4) and Equivalent Isotropic Displacement Parameters ($Å^2$ × 10^3) for the Complex

Atoms	x	y	z	U(eq)
C(1)	2235(2)	1240(7)	635(2)	36(1)
C(2)	1479(2)	1305(8)	531(2)	47(1)
C(3)	1191(2)	1471(8)	−243(3)	55(1)
C(4)	1643(3)	1595(8)	−908(3)	63(2)
C(5)	2400(2)	1540(8)	−815(2)	51(1)
C(6)	2700(2)	1368(7)	−35(2)	37(1)
N(7)	3465(2)	1321(6)	73(2)	41(1)
C(8)	3777(2)	1126(7)	819(2)	41(1)
C(9)	3273(2)	989(7)	1547(2)	38(1)
N(10)	2540(2)	1064(6)	1422(2)	38(1)
C(11)	3962(2)	1442(8)	−636(2)	61(2)
O(12)	4442(1)	1101(5)	932(2)	60(1)
O(13)	3544(2)	798(5)	2230(2)	55(1)
C(14)	2054(2)	935(7)	2140(2)	47(1)
I(1)	0	800(1)	2500	58(1)
K(1)	5000	809(3)	2500	56(1)

U(eq) is defined as one third of the trace of the orthogonalized Uij tensor.

hydrogen atoms were allowed to ride on the parent atoms in the model. Refinements were carried out using SHELXL-97.[10] Molecular structures were drawn using ORTEP and Material studio software.[11]

2.3. Spectroscopy Measurements

Electronic absorption and fluorescence spectra in various solvents have been recorded at room temperature. All the used solvents are commercial and of

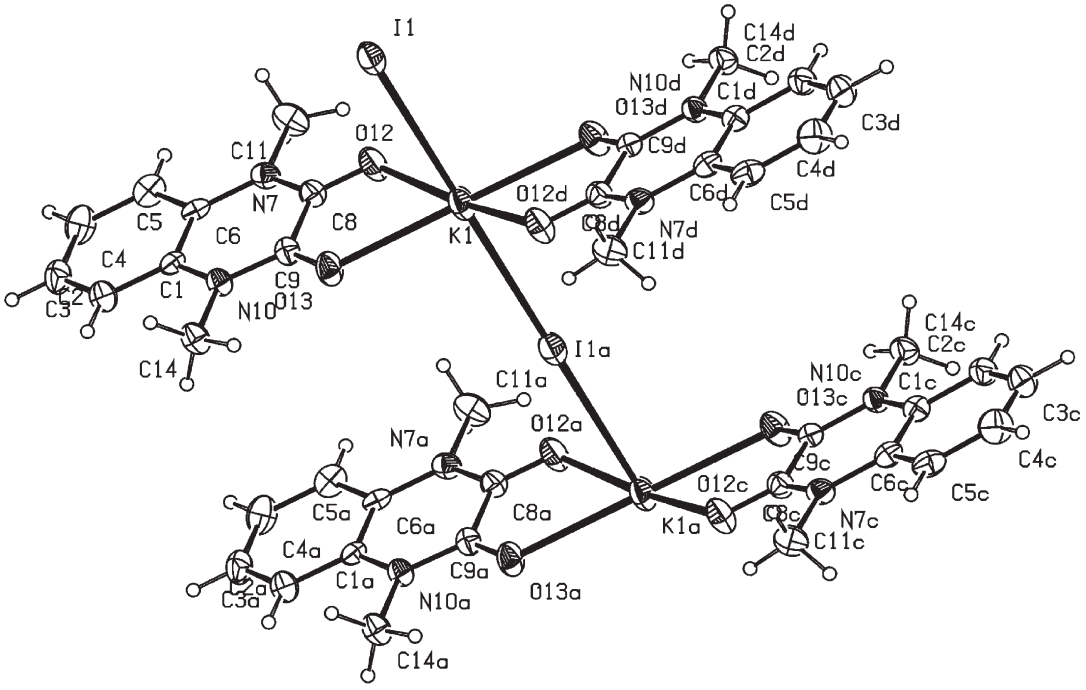

FIGURE 3 ORTEP Drawing of the Complex Showing the Atom Numbering Scheme and Thermal Motion Ellipsoids (50% Probability Level for Non-hydrogen Atoms).

TABLE 3 Bond Lengths (Å) and Angles (Degrees)

C(1)-C(6)	1.389(5)	C(3)-C(4)	1.368(6)	C(8)-C(9)	1.508(5)
C(1)-C(2)	1.388(5)	C(5)-C(6)	1.395(5)	I(1)-K(1)#1	3.540(3)
C(2)-C(3)	1.378(5)	C(4)-C(5)	1.386(6)	K(1)-I(1)#1	3.554(3)
C(1)-N(10)	1.410(4)	C(6)-N(7)	1.405(5)	O(13)-K(1)	2.688(3)
N(10)-C(14)	1.475(4)	N(7)-C(11)	1.473(4)	O(12)-K(1)	2.770(3)
C(9)-N(10)	1.350(4)	N(7)-C(8)	1.356(5)	K(1)-C(9)#3	3.514(3)
C(8)-O(12)	1.224(4)	C(9)-O(13)	1.231(4)	K(1)-C(8)#3	3.548(3)
C(14)-I(1)	3.787(5)	I(1)-C(14)	3.540(3)	K(1)-C(11)#4	3.931(3)
C(6)-C(1)-C(2)	120.4(4)	C(6)-C(1)-N(10)	119.2(3)	C(2)-C(1)-N(10)	120.4(3)
C(3)-C(2)-C(1)	119.5(4)	C(4)-C(3)-C(2)	120.7(4)	C(3)-C(4)-C(5)	120.5(4)
C(4)-C(5)-C(6)	119.5(4)	C(1)-C(6)-C(5)	119.4(4)	C(1)-C(6)-N(7)	120.3(3)
C(5)-C(6)-N(7)	120.3(3)	C(8)-N(7)-C(6)	122.1(3)	C(8)-N(7)-C(11)	117.3(3)
C(6)-N(7)-C(11)	120.6(3)	O(12)-C(8)-N(7)	123.5(3)	O(12)-C(8)-C(9)	118.8(3)
N(7)-C(8)-C(9)	117.7(3)	N(10)-C(9)-C(8)	118.7(3)	C(9)-N(10)-C(1)	122.1(3)
O(13)-C(9)-C(8)	118.8(3)	O(13)-C(9)-N(10)	122.5(3)	C(1)-N(10)-C(14)	119.9(3)
O(13)-C(9)-K(1)	39.9 (2)	C(8)-C(9)-K(1)	79.0(2)	C(9)-N(10)-C(14)	118.0(3)
N(10)-C(9)-K(1)	162.3(2)	C(9)-O(13)-K(1)	123.0(3)	O(13)#3-K(1)-C(9)	162.95(8)
O(12)#3-K(1)-O(12)	171.4(2)	O(13)-K(1)-C(9)	17.09(8)	O(12)-K(1)-C(9)	41.99(8)
O(13)#3-K(1)-O(13)	179.6 (2)	O(13)-K(1)-O(12)	59.05(8)	O(13)-K(1)-O(12)#3	120.98(8)
K(1)#1-I(1)-K(1)#2	180.0	O(12)#3-K(1)-C(9)	137.55(8)	O(13)#3-K(1)-I(1)#2	90.18(8)
O(13)-K(1)-C(9)#3	162.95(8)	O(12)#3-K(1)-C(9)#3	41.99(8)	O(12)#3-K(1)-I(1)#2	85.72(9)
C(9)-K(1)-C(9)#3	175.8 (2)	C(9)-K(1)-I(1)#2	87.92(9)	O(13)#3-K(1)-I(1)#1	89.82(8)
O(12)#3-K(1)-I(1)#1	94.28(9)	C(9)-K(1)-I(1)#1	92.08(9)		

Symmetry transformations used to generate equivalent atoms: #1, $-x+1/2, y-1/2, z$; #2, $-x+1/2, y+1/2, z$; #3, $-x+1, y, -z+1/2$; and #4, $x, -y, z+1/2$.

spectroscopy grade. Experimental technique and apparatus for measurements are described elsewhere.[12]

3. RESULTS AND DISCUSSIONS

3.1. Crystal Ddata of the Complex

The 1,4-dimethylquinoxaline-2,3-dione potassium iodide complex structure has been determined at room temperature. The details of structure analysis are given in Table 1 and the ORTEP plot of the complex is given in Figure 3. The complex crystallizes in orthorhombic Pbcn group and contains eight molecules. The atomic coordinates and equivalent isotropic displacement parameters of the atoms are given in Table 2. Bonds lengths and angles are given in Table 3. The phenyl group presents standard C–C bond lengths about 1.39 Å. N(7)–C(8) and N(10)–C(9) distances are shorter than C(6)–N(7) and C(1)–N(10) indicating a slight resonance with the O(12) and O(13), respectively, which is coherent with the delocalization of the carbonyl double bond. The N(7)–C(11) and N(10)–C(14) distances are in agreement with the theoretical studies of some heterocyclic derivatives previously done by some of us.[13–15] Each potassium atom has a dative bond with four oxygen. Close contacts involving the K atom can be noticed as K(1)–C(9)#3 (3.514 Å), K(1)–C(8)#3 (3.548 Å), K(1)–C(11)#4 (3.931 Å), and I(1)–K(1)#1 (3.540 Å) (Table 3). Moreover, the distances between the K atom and the two oxygen atoms are slightly different: 2.770 Å for O(12)–K(1) and 2.688 Å for O(13)–K(1). These values indicate some geometric deformation in the complex structure. Furthermore, two intramolecular hydrogen bonding chelate withdrawals appear involving C(11)–H(11A)···O(12) and C(14)–H(14C)···O(13);

TABLE 4 Intramolecular Hydrogen Bonding with Chelate Withdrawal Geometry

D	H	A	D–H (Å)	H...A (Å)	D...A (Å)	D–H...A (°)
C11	H11A	O12	0.9597	2.2948	2.725(5)	106.32
C14	H14C	O13	0.9599	2.2741	2.718(5)	107.21

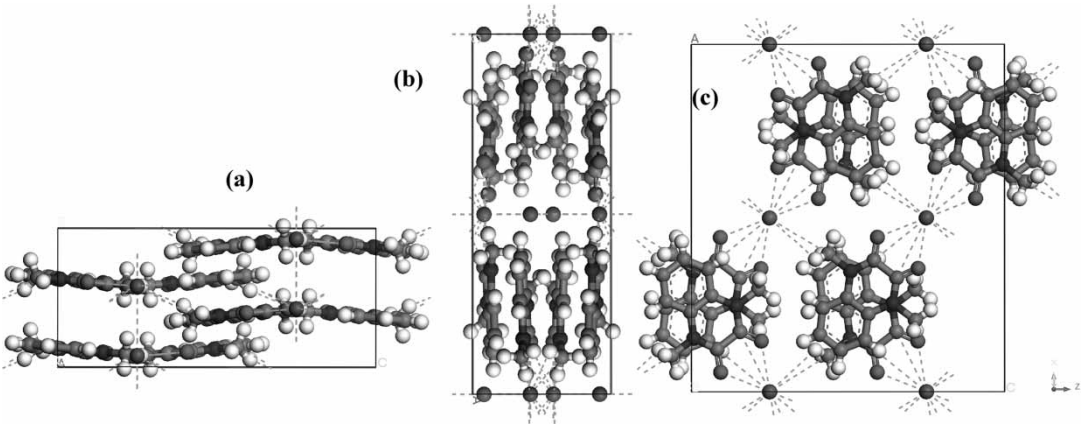

FIGURE 4 **Projection of the Complex Crystal Structure: (a) Along a, (b) Along c, and (c) Along.**

bond length and angles are given in Table 4. The projections of the crystal structure along a, c, and b are plotted in Figures 4a, 4b, and 4c, respectively. The 1,4-dimethylquinoxaline-2,3-dione molecules are set along two rows parallel to the b axis and separated by straight lines containing alternately the potassium and iodine atoms that are located on a twofold axis parallel to b and situated at $z = 0.25$. The two rings of the 1,4-dimethylquinoxaline-2,3-dione molecules are nearly in the same plane. The molecules are not parallel one to another and do not show π-π intermolecular interaction.

3.2. Spectroscopy Analysis

3.2.1. *Electronic Absorption*

In Figure 5 are reported the room temperature absorption spectra of the 1,4-dimethylquinoxaline-2,3-dione potassium iodide complex and the 1,4-dimethylquinoxaline-2,3-dione molecule in solution at concentration $C = 10^{-4}$ M. As is shown in this figure, a resemblance appears at the level of the structure and form of the two spectra absorption; the only difference appears in their maximum position. The energy band difference is estimated to be 1700 cm^{-1} indicating more stability of the complex than the molecule in the ground state. This observation suggests the existence in solution of two absorbent entities, which are the complex and the 1,4-dimethylquinoxaline-2,3-dione molecule.

Figure 6 reports the room temperature absorption spectra of the 1,4-dimethylquinoxaline-2,3-dione potassium iodide complex in solution at concentration $C = 10^{-4}$ M. The spectrum in each solvent presents one dominant high-intensity band with two shoulders that appear on the long wavelength tail of the intense peak. The highest energy band, which is the most intense, is located in *n*-hexane at around 284 nm, and the lowest energy bands at shoulders are located at 297 and 317 nm. The band is red-shifted by

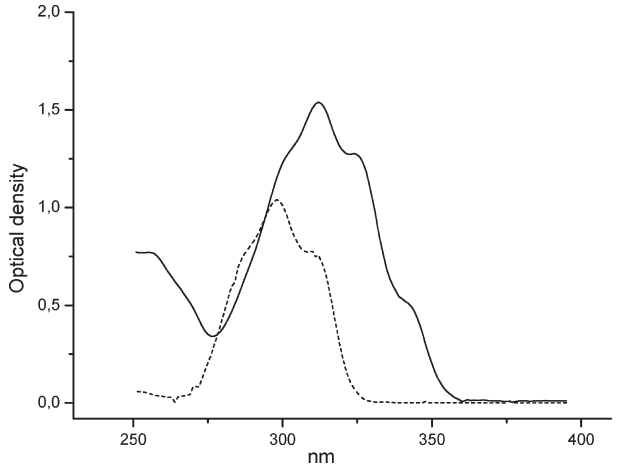

FIGURE 5 **Absorption Spectra in Ethanol of the 1,4-Dimethylquinoxaline-2,3-Dione (...) and the Complex (___) at Room Temperature ($C = 10^{-4}$ M).**

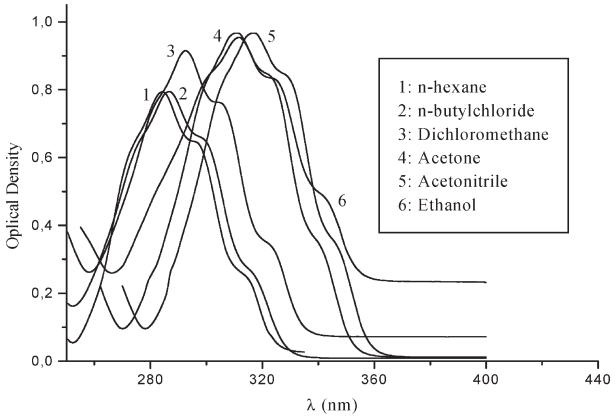

FIGURE 6 **Absorption Spectra in Different Solvents of the Complex at Room Temperature ($C = 10^{-4}$ M).**

TABLE 5 Absorption ν_a, Fluorescence Maxima ν_f and $\Delta\nu_{st}$ of the Complex in Different Solvents as a Function of $\Delta f(D,n)$ at Room Temperature

Solvent	$\Delta f\,(D,n)$	ν_a (cm^{-1})	ν_f (cm^{-1})	$\Delta\nu_{st}$ (cm^{-1})
n-Hexane	0.003	35,211	22,935	12,276
N-Butylchloride	0.209	34,843	24,203	10,640
Dichloromethane	0.215	34,722	24,402	12,320
Acetone	0.246	32,362	22,537	9825
Acetonitrile	0.306	32,453	22,522	9637
Propanol	0.262	32,467	23,584	8883
Butanol	0.276	32,368	23,529	8333
Ethanol	0.289	32,348	23,568	8780
Methanol	0.311	32,051	23,310	8741

about 33 nm when the solvent polarity is increased from *n*-hexane ($\mu = 0.0$ D) to acetonitrile ($\mu = 3.4$ D). The important red shift caused by the solvent polarity effect led us to attribute the two low-intensity bands to a $\pi\pi^*$ transition. The band at 284 nm corresponds with the ^1L_b transition of the phenyl part. The important red shift provokes a high stabilization of the complex in the ground state in polar solvents. This stabilization can be mainly due to the electronic polarization effect of the solvent. The corresponding state is considered as a CT (charge transfer) state created by dipole–dipole interactions.

On the other hand, the absorption band spectra of the complex are critically dependent on the nature of the solvent. In fact, as shown in Figure 4 and Table 5, the shift due to the polarity effect in a protic solvent such as ethanol ($\mu = 1.7$ D) appears larger than the shift obtained in an aprotic solvent such as *n*-butylchloride ($\mu = 1.9$ D). This observation indicates that the shift in ethanol is due to two simultaneous effects that should be identified as the solvent polarity and the hydrogen bonding interaction. The hydrogen bonding energy of the complex is evaluated by using the data in Table 4. As a consequence, the obtained value for the hydrogen bonding energy is estimated to be 2500 cm^{-1} and the dipole–dipole interaction energy is about 300 cm^{-1} in ethanol. Comparison of theses values indicates that the strong hydrogen bonding effect exerts a specific influence on the complex and reduces the magnitude of the CT interactions within the complex. It should be noted that the hydrogen bonding complex was formed between the hydroxyl group of alcohol and the π electron of the molecule ring (OH...π) type or the oxygen of the C=O group (O...HO).

3.2.2. Electronic Emission

Figure 7 collects the fluorescence spectra of the complex in the same solvents used for absorption study. This figure shows that the fluorescence band structures are strongly dependent on the nature of the solvent. Indeed, in aprotic solvents the spectrum has a large band with a maximum at about 436 nm in *n*-hexane. This band is red-shifted on going from the nonpolar *n*-hexane to polar acetonitrile solvents. The red shift evaluated to 420 cm^{-1} stabilizes the complex in the first excited state. This stabilization is weaker than in the ground state. Furthermore, it should be noted (Table 5) that the calculated Stokes shift in these solvents is found to be very large. This phenomenon is attributed to a change in geometric conformation of the complex between the ground and excited states. The dipole moment orientation of the complex excited state is not identical to this in the ground state.

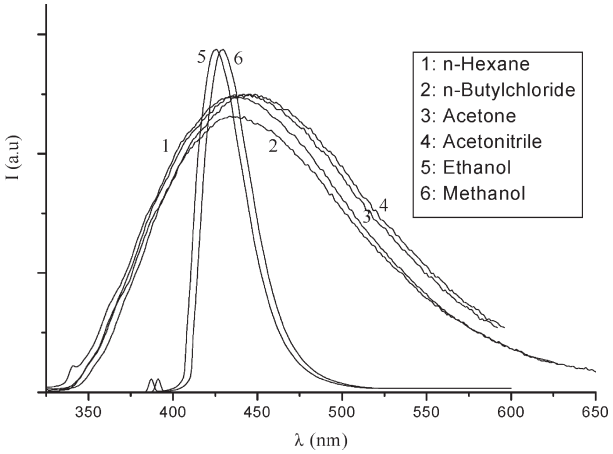

FIGURE 7 Fluorescence Spectra of the Complex in Different Solvents at Room Temperature λ_{exc} = 300 NM, (C= 10^{-4} M).

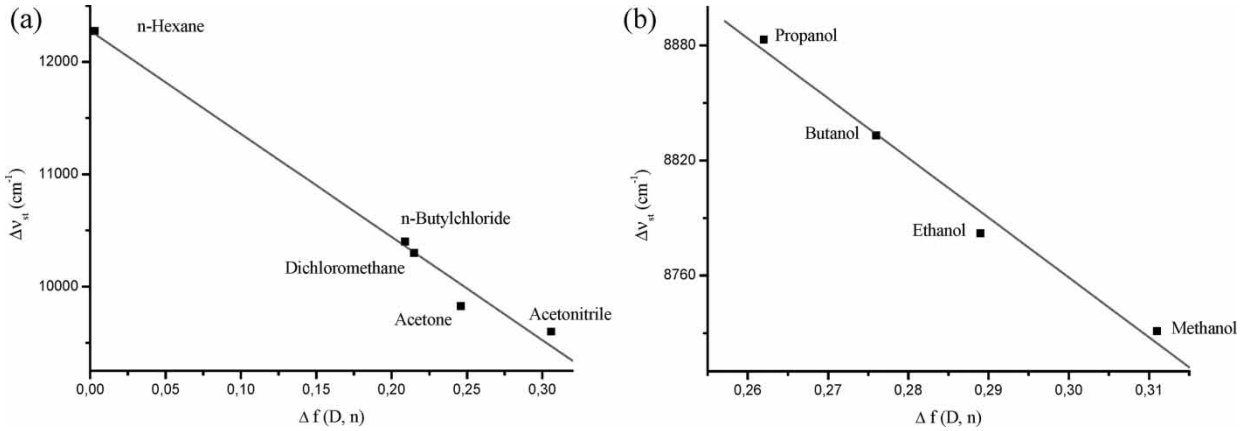

FIGURE 8 **Evolution of $\Delta\nu_{st}$ According to $\Delta f(D,n)$ for the Complex (Correlation Factors R = 99%). (a) in Aprotic Solvents, (b) in Protic Solvents.**

The spectral behavior of the complex presents a remarkable change in the protic solvents. The fluorescence band appears, and its maximum is blue-shifted with increasing solvent polarity. This anomaly is due to a hydrogen bonding effect on the complex in its excited state. Contrary to dipole–dipole interactions that stabilize the complex in this state, the hydrogen bonding contributes strongly in its destabilization. The higher stability of the complex can be explained by the larger dipole moment in polar and aprotic solvents compared with that in protic solvents.

The fluorescence band as discussed before is critically dependent on the solvent polarity and on the hydrogen bonding effects. The electrostatic and charge transfer interactions in aprotic and polar solvents influence the geometry of the complex in its S1 (CT) excited state. The difference of the geometry in this state and the state in protic solvent implies a difference in their dipole moment. In order to estimate this difference, we have determined the Stokes shift as a function of the solvent macroscopic features (Table 5). The difference ($\Delta\mu$) between the excited and the ground states is determined in protic and aprotic solvents.

According to Lippert and Mataga[16,17] formalisms, the Stokes shift is given by the relation (1),

$$\Delta\nu_{\mathrm{st}} = (\nu_a - \nu_f) = m\Delta f\,(D, n) \qquad (1)$$

where $\Delta f(D,\ n) = [(D-1)(2D+1)^{-1}] - [(n^2-1)(2n^2+1)^{-1}]$; in this expression, n and D[18,19] designate respectively the relative index and the static dielectric constant of the solvents. m is given by Equation (2)

$$m = 2(\mu_e - \mu_g)^2/hca^3, \qquad (2)$$

where μ_e and μ_g are the dipole moments of the complex in the excited and ground states, a designates the Onsager cavity radius, h Planck's constant, and c the speed of light in a medium. This relation is applied in the two following cases. We note that $(\Delta\mu)_a = \mu(\mathrm{CT}) - \mu_g$ in aprotic solvents and $(\Delta\mu)_p = \mu(\pi\pi^*)\text{-}\mu_g$ in protic solvents. Figure 8 shows a linear regression (origin program) of $\Delta\nu_{st}$ as a function of $\Delta f(D,n)$. This causes us to determine two slopes for the complex.

The first slope (Fig. 8a) equal to 9176 cm^{-1} gives the difference of the dipole moment between the ground S1 (CT) excited state. The second slope (Fig. 8b) equal to 3118 cm^{-1} gives the difference between the ground state and the S1 ($\pi\pi^*$) excited state. The use of this curve gives a $(\Delta\mu)_a/(\Delta\mu)_p$ ratio equal to 3. This result shows a noticeable difference in dipole moment of the complex between the protic and aprotic solvents.

4. CONCLUSIONS

1,4-Dimethylquinoxaline-2,3-dione potassium iodide complex was prepared and characterized by single X-ray structure. Its crystal structure has been solved at room temperature. A detailed description of the geometry of the 1,4-dimethylquinoxaline-2,3-dione in the K and I positions has been given. Moreover, the results obtained in the study by UV spectroscopy in aprotic and protic solvents confirm the important role played by the dipolar and hydrogen bonding interactions in the nature of photophysical properties of the complex. Indeed, the comparison of the $\Delta\mu$ values estimated for the series of solvents are not the same, a fact that is compatible with the remarkable difference in the absorption and emission found in the two types of media.

ACKNOWLEDGMENTS

This work has been supported by the French-Morocco cooperation CNRS/CNRST N°18606.

REFERENCES

1. Cheeseman, G. W. H.; Cookson, R. F. *Condensed Pyrazines. The Chemistry of the Heterocyclic Compounds*; New York, 1979, 35; 78–111.
2. Ohmori, J.; Sakamoto, S.; Kubota, H.; Shimizu-Sasamata, K.; Okada, M.; Kawasaki, S.; Hidaka, K.; Togami, J.; Furuya, T.; Murase, K. *J. Med. Chem.* **1994,** *37*, 467–475.
3. Gerothanassis, I. P.; Vakka, C. *J. Org. Chem.* **1994,** *59*, 2341–2348.
4. Webb, G. A. In *The Multinuclear Approach to NMR Spectroscopy*; Lambert, J. B., and Riddell, F. G. Eds.; D. Reidel: Dordrecht, 1983.
5. Honore, T.; Davis, S. N.; Drejer, J.; Fletcher, E. J.; Jacobson, P.; Lodge, D.; Nielson, F. E. *Science* **1988,** *241*, 701–703.
6. Honore, T.; Drejer, J.; Jacobsen, P.; Nielsen, F. E.E.R. Patent. Application 260467, 1988.
7. Foster, A. C. *Nature* **1988,** *335*, 669–670.
8. Tanaka, K.; Takahah, H.; Masahiko Sugita, K.-T.; Mitsuhashi, K. *J. Heterocyclic Chem.* **1992,** *29*, 771.
9. Shu-Kun. *Flax Molecules* **1996,** *1*, 37.
10. Sheldrick, G. *SHELXS-97 Program for the refinement of Crystal Structure*; University of Göttingen: Göttingen, Germany, 1997.
11. MS Modeling (Material Studio) 3.0. Available at http://www.accelrys.comcom/mstudio/ ms_modeling/.
12. Lazar, Z.; Benali, B.; Elblidi, K.; Zenkouar, M.; Lakhrissi, B.; Massoui, M.; Kabouchi, B.; Cazeau-Dubroca, C. *J. Mol. Liq.* **2003,** *106*, 89–95.
13. Pacios, L. F.; Lazar, Z.; Benali, B. J. *Mol. Struct. (Theochem).* **2002,** *594*, 89–100.
14. Mondieig, D.; Ph Négrier; Léger, J. M.; Benali, B.; Lazar, Z.; El Assyry, A.; Lakhrissi, B.; Massoui, M. *M. Anal. Sci.* **2005,** *21* (19), 145.
15. Ph Négrier; Mondieig, D.; Léger, J. M.; Benali, B.; Lazar, Z.; Boucetta, A.; Elassyry, A.; Lakhrissi, B.; Jermoumi, C.; Massoui, M. *Anal. Sci.* **2006,** *22* (7), 175.
16. Lippert, E. Z. *Naturforsch, A.* **1955,** *10a*, 541.
17. Mataga, N.; Keifu, Y.; Koizumi, M. *Bull. Chem. Soc. Jpn.* **1986,** *29*, 465.
18. Riddick, J. A.; Bunger, W. R. *Techniques of Chemistry*; Weissberger, A., Ed.; Wiley Interscience: New York, 1970.
19. Weast, R. C., Ed.; *Handbook of Chemistry and Physics*, 52nd Edn.; (1971–1972) and 61st Edn; (1980–1981), CRC Press: Boca Raton.